

Experimental study and exergy analysis of photovoltaic-thermoelectric with flat plate micro-channel heat pipe

 The corrections made in this section will be reviewed and approved by journal production editor.

Samson **Shittu** Writing - review & editing Writing - original draft Investigation Conceptualization ^a,
Guiqiang **Li** Project administration Writing - review & editing Investigation ^{a,*} Guiqiang.Li@hull.ac.uk,
Xudong **Zhao** Funding acquisition ^{a,*} Xudong.Zhao@hull.ac.uk, Jinzhi **Zhou** Investigation ^b, Xiaoli **Ma**
Supervision ^a, Yousef Golizadeh **Akhlaghi** Investigation ^a

^aCentre for Sustainable Energy Technologies, University of Hull, HU6 7RX, UK

^bSchool of Mechanical Engineering, Southwest Jiaotong University, Chengdu, Sichuan, PR China

*Corresponding authors.

Abstract

Effective cooling of the photovoltaic can enhance electrical conversion efficiency of a photovoltaic system. The combination of photovoltaic and thermoelectric generator provides unique advantages because of their complementary characteristics. In addition, hybrid photovoltaic-thermoelectric can utilize a wider solar spectrum thereby harvesting more energy from the sun. Heat pipes are passive devices that can transfer heat efficiently over a long distance. Therefore, this study presents an experimental investigation and exergy analysis of a photovoltaic-thermoelectric with flat plate micro-channel heat pipe. The experiment is performed in a laboratory using a solar simulator and water-cooling is used for the thermoelectric generator. The effect of thermoelectric load resistance, micro-channel heat pipe back insulation and solar radiation on the performance of the hybrid system is presented and a comparison with a photovoltaic only system is provided. Results show that the hybrid system provides an enhanced performance compared to the photovoltaic only system and absence of insulation behind the micro-channel heat pipe enhances electrical performance of the hybrid system. Furthermore, results show the feasibility of the hybrid system for generating electricity and small hot water. This study will provide valuable guidance for design of photovoltaic-thermoelectric systems with heat pipe and verifies the feasibility of such systems.

Keywords: Photovoltaic-thermoelectric; Micro-channel heat pipe; Exergy; Thermal management; Power generation

Nomenclature

A	Area of PV cell, m ²
A _c	Area of PV collector, m ²
c _w	Specific heat capacity, J/kg/°C
G	Solar radiation, W/m ²
I	Current, A
m	Mass, kg
P	Power output, W
Q̇ _{th}	Water heating capacity, J
T	Temperature, °C
\bar{T}	Average temperature, °C

Greek symbols

$\varphi_{\text{srad,max}}$	Maximum efficiency ratio
η	Efficiency, %

Abbreviations

MCHP	Micro-channel heat pipe
PV	Photovoltaic
PV-TE	Photovoltaic-thermoelectric
TE	Thermoelectric
TEG	Thermoelectric generator

Subscripts

a	Ambient
sun	Sun
w _{tank}	Water tank

1 Introduction

Environmental problems such as global warming and air pollution are caused by the use of conventional energy sources like fossil fuel therefore, clean and renewable energy sources are attracting greater attention [1]. Solar energy which is free and inexhaustible is one of the most promising renewable energy solution to reduce fossil fuel consumption and abate negative environmental issues [2]. Photovoltaic (PV) is one of the most mature solar energy conversion technologies which converts sunlight directly into electricity with little need for maintenance, silent operation and absence of moving parts [3]. However, the main drawback of the

PV is its low conversion efficiency [4]. Consequently, a great percentage of the absorbed solar energy by the photovoltaic is converted into heat, which increases the temperature of the PV and thus, leads to a decrease in the efficiency because of the negative performance temperature coefficient [5]. The wider adoption of photovoltaic technology on a global scale is dependent on a significant increase in the conversion efficiency of the PV therefore, research on effective management of the waste heat from the PV is being paid more attention [6].

Thermoelectric generator (TEG) is one of the most attractive waste heat recovery technologies [7] because of its unique advantages such as zero emission, solid-state operation, silent operation, absence of moving parts, high reliability and maintenance free operation [8]. A thermoelectric generator is a solid-state device which can generate electricity directly from heat via the Seebeck effect [9]. However, the widespread application of thermoelectric generators has been hindered by their low conversion efficiency [10]. However, the efficiency of thermoelectric generators can be improved through geometry optimization and material optimization [11]. In addition, the use of thermoelectric generators in a hybrid system can enhance its performance [12]. In recent years, research on hybrid photovoltaic-thermoelectric (PV-TE) has accelerated faster than other hybrid photovoltaic technologies due to its huge potential [13]. While the photovoltaic utilizes the visible and ultra-violet regions of the solar spectrum, the thermoelectric utilizes the infrared region [14]. Therefore, integration of the photovoltaic and thermoelectric will lead to a more efficient and broader utilization of the solar spectrum [15].

The two main methods for integrating the photovoltaic and thermoelectric are spectrum splitting and direct coupling methods [16]. The spectrum splitting method involves the use of a reflective component, such as beam splitter or prism. Radiation longer than the cut-off wavelength is reflected to the thermoelectric generator while those shorter than the cut-off wavelength is transmitted through the splitter and absorbed by the photovoltaic [17]. The direct coupling method does not need the use of a splitter rather; the TEG is placed directly behind the PV in a parallel arrangement. Consequently, the total cost of the system for direct coupling PV-TE system would be lower than that for spectrum splitting PV-TE system due to the absence of additional components like beam splitter. In addition, the direct coupling PV-TE systems are less complicated compared to the spectrum splitting PV-TE systems, as the system configuration only requires parallel arrangement of the photovoltaic and thermoelectric generator. Yin et al. [18] presented a novel optimal design method for a concentrated photovoltaic-thermoelectric (CPV-TE) system using the spectrum splitting method. The effects of thermoelectric figure of merit and cooling system convective heat transfer coefficient on the optimal system design were studied and the optimal cut-off wavelength of the spectral splitter was provided. Results revealed that the cooling system convective heat transfer coefficient does not significantly influence the optimal cut-off wavelength when the thermoelectric figure of merit is small. On the other hand, direct coupling method was used by Li et al. [19] to investigate the optimum thermoelectric load resistance in a photovoltaic-thermoelectric system. An inconsistency in the optimum thermoelectric load resistance in a thermoelectric (TE) only and PV-TE was observed therefore, the authors argued that the thermoelectric load resistance for obtaining maximum power output from the TE only is different from that for the PV-TE.

There is a plethora of literatures on numerical study of photovoltaic-thermoelectric however; literatures on experimental investigation of PV-TE are limited. Babu and Ponnambalam [20] investigated the performance of

a non-concentrated flat plate photovoltaic-thermoelectric and results showed that the hybrid system provided an efficiency increase of 6%. However, only a theoretical study was carried out and a non-practical assumption of thermoelectric generator cold side temperature being constant was used in the analysis. Mahmoudinezhad et al. [21] presented a transient model for a concentrated photovoltaic-thermoelectric and finite volume method was used to study the performance of the hybrid system. Results showed that the presence of thermoelectric generator in the hybrid system could stabilize the temperature fluctuation due to solar radiation variation. However, the authors used an unsteady-state one-dimensional heat transfer model to perform the transient study. Zhang et al. [22] demonstrated the suitability of polycrystalline silicon thin-film photovoltaic cell for CPV-TE system using a theoretical model. In addition, they found that the polymer photovoltaic cell is best suited for non-concentrated hybrid photovoltaic-thermoelectric systems. The results obtained from in this study were from the theoretical model used and experiment was not performed.

Furthermore, Singh et al. [23] performed an energy and exergy analysis of a concentrated photovoltaic-thermoelectric system and results showed that the irreversibility increases with increase in concentration ratio. The authors assumed that the TEG attached to the backside of the PV obtained the entire waste heat from the photovoltaic with no heat loss through convection, radiation or conduction to the environment at the PV backside. Rezania et al. [24] proved the feasibility of CPV-TE system considering different solar concentrations and heat sink types. Results showed that the hybrid system provided an enhanced performance compared to the concentrated PV only system. However, the authors neglected the effect of natural convection and force convection over the glass cover of the system. In addition, only a theoretical feasibility study was provided and not an experimental feasibility study. Fallan Kohan et al. [25] presented a three-dimensional numerical study of a PV-TE using finite volume method. Results showed that the contribution of the TEG to the overall power output becomes significant at high concentrations. However, this study was carried out under the assumption of steady state conditions and not transient conditions. In addition, the optical efficiency of the solar concentrator used was assumed perfect. Motiei et al. [26] investigated the performance of a hybrid photovoltaic-thermoelectric system using a transient two-dimensional model. They observed a 0.59% and 5.06% increase in the PV efficiency and electrical power output respectively. However, the authors provided no experimental validation. Li et al. [27] found that high concentration ratio and appropriate PV cell used in a hybrid PV-TE system could enhance the system output efficiency. This study was performed using a one-dimensional model based on the laws of thermodynamics. Yang et al. [28] found that the spectrum splitting PV-TE system provided a 2.67% and 2.19% efficiency increase at concentration factors of 30 and 100 respectively compared to the single PV cell.

Kossyvakis et al. [29] presented an experimental investigation of the performance of a photovoltaic-thermoelectric using polycrystalline silicon cell and dye-sensitized solar cell. In addition, thermoelectric geometry optimization was performed, and the results revealed that thermoelectric generators with shorter legs are provide enhanced overall hybrid system performance due to reduced PV operating temperature. Zhang et al. [30] experimentally demonstrated the feasibility of a new design for photovoltaic-thermoelectric without thermoelectric generator ceramic plates in order to reduce thermal resistance. The authors argued that their new design increased the efficiency of the PV and TE because of better heat transfer. Cui et al. [31] presented an experimental study of a novel photovoltaic-thermoelectric with phase change material (PCM). The function of the PCM was to regulate the system temperature and a comparison was made with a PV only system.

Results revealed that the hybrid system efficiency using water-cooling was higher than that with air-cooling under the same environmental conditions.

Similarly, Darkwa et al. [32] presented an experimental and numerical study of a photovoltaic-thermoelectric with phase change material. Unlike the research of Cui et al. [31] where the PCM was positioned between the PV and TEG, the authors positioned the PCM at the bottom of the TEG. Results revealed that the thicker PCM layers could effectively lower the photovoltaic temperature for a longer period although the PCM also acts as an insulator thereby reducing power output. However, the authors argued that the hybrid system with PCM provided an enhanced power output of 9.5% compared to the hybrid system without PCM and PV only system during an initial 1.5 h period. Furthermore, Mahmoudinezhad et al. [33] performed an experimental and numerical study on a transient behaviour of photovoltaic-thermoelectric with multi-junction solar cell. A solar simulator was used to vary the concentrated solar radiation and results indicated that the thermoelectric generator stabilizes the power output of the hybrid system. Recently, Yin et al. [34] demonstrated the feasibility of concentrated photovoltaic-thermoelectric experimentally. A comparison with PV only system was made under varying optical concentration ratio and the influence of thermoelectric thermal resistance was studied. Results showed that the hybrid system provided a superior performance compared to the PV only system.

Heat pipes are efficient heat transfer devices capable of transporting heat over a distance with a small temperature gradient using the principle of latent heat of vaporisation [35]. Flat plate microchannel heat pipe (MCHP) provides better performance due to its enhance heat transfer capabilities because of its micro-channel structure, therefore, it is one of the most preferred heat pipes currently [36]. The integration of heat pipes with thermoelectric generators has been researched recently. Lv et al. [37] investigated a high-performance solar thermoelectric system with micro-channel heat pipe for combined heat and power. They found that the new system achieved a thermal efficiency greater than 57% and an electrical efficiency above 3% at a solar irradiation greater than 700 W/m^2 . Li et al. [38] studied a solar concentrating TEG system with micro-channel heat pipe array. They found that the new system provided a greater power output and lower cost compared to the solar TEG.

Similarly, Makki et al. [39] presented a numerical study of a photovoltaic-thermoelectric with heat pipe. A mathematical model based on energy balance was used to evaluate the performance of the hybrid system and the authors argued that the hybrid system with heat pipe could be used in sunny regions with high operating temperature. However, the aluminium heat spreaders used to increase the area of the heat pipe evaporator section could introduce additional thermal losses. Furthermore, Li et al. [40] presented a photovoltaic-thermoelectric system with flat plate micro-channel heat pipe. The annual performance and economic analysis of the new system was presented and a comparison with PV only system was made. The authors argued that the use of micro-channel heat pipe could reduce the number of thermoelectric generators needed significantly compared to conventional photovoltaic-thermoelectric system. However, the thermoelectric generator was cooled using heat sink air-cooling which is not a very effective cooling method compared to water-cooling. Shittu et al. [41] presented a three-dimensional study of a PV-TE with flat plate heat pipe using finite element method. Results showed that ineffective cooling of thermoelectric generator could negatively affect the

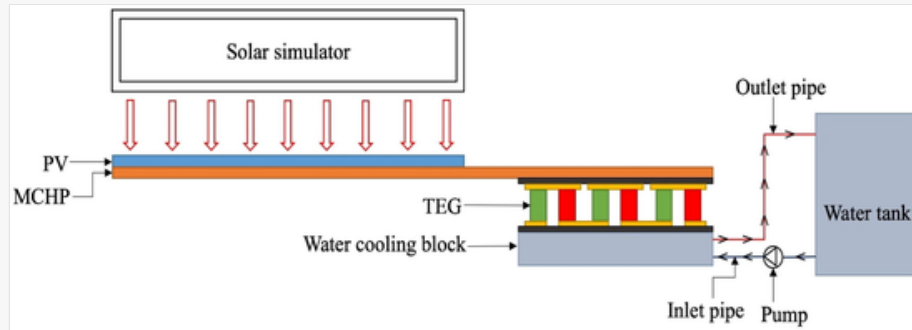
performance of the hybrid system. However, the authors did not provide experimental validation of the numerical results.

The literature review above has demonstrated the feasibility of photovoltaic-thermoelectric with heat pipe however; there is a lack of experimental validation. In fact, the reported experimental literatures are on photovoltaic-thermoelectric without heat pipe. The significance of experimental studies is that numerical simulation is often performed under ideal conditions whereas experimental studies provide a true reflection of the system performance under real conditions, which can then be used for further system optimization. Furthermore, it has been shown that water-cooling of thermoelectric generator is better than air-cooling. However, there is currently no study on photovoltaic-thermoelectric heat pipe with water-cooling. Therefore, for the first time, this study presents a detailed experimental investigation of a photovoltaic-thermoelectric with flat plate micro-channel heat pipe and water-cooling of the thermoelectric generator. In addition, the feasibility of the hybrid system for power generation and hot water production is demonstrated for the first time. The experimental study is conducted in a laboratory therefore; a solar simulator is used to vary the solar radiation. The effect of insulation layer on the backside of the flat plate micro-channel heat pipe on the performance of the hybrid system is investigated and a comparison with a PV only system is made. Furthermore, the energy and exergy analysis of the hybrid system under varying solar radiation is performed and temperature distribution in the hybrid system is presented.

2 System description and operation

The structure of the photovoltaic-thermoelectric-microchannel channel heat pipe (PV-TE-MCHP) system considered in this study is shown in Fig. 1. The hybrid system consists of photovoltaic (PV), thermoelectric generator (TEG), flat plate microchannel heat pipe (MCHP), water-cooling block, pump and water tank as shown in Fig. 1. The PV absorbs solar energy from the solar simulator and converts a part of this solar energy into electricity while the remaining is converted into thermal energy. The flat plate microchannel heat pipe is attached directly behind the PV in such a way that the PV is placed at the top of the MCHP evaporator. Thermal energy from the PV is transferred to the MCHP through its evaporator and this energy is transported to the condenser of the MCHP via evaporation of the working fluid inside the MCHP. Subsequently, heat (thermal energy) is released from the condenser of the MCHP via condensation of the working fluid in the micro-channel heat pipe and this heat is transferred to the thermoelectric generator, which is attached to the bottom of the MCHP condenser. A water-cooling block is placed on the cold side of the TEG to cool the thermoelectric generator therefore; a temperature difference is achieved across the TEG due to the heat from the MCHP condenser and the water cooling at the bottom of the TEG. Therefore, the TEG generates additional electricity via the Seebeck effect. A pump is used to circulate the water and it ensures the cooling water flows through the cooling block using the inlet and outlet pipes. During the system operation, the heat removed from the TEG will increase the temperature in the water tank and the total volume of cooling water is constant throughout system operation. The dimensions of the main system components are shown in Table 1. The area of the water-cooling block and the TEG is the same thereby enhancing the cooling effectiveness. Throughout the system operation, the flow rate is maintained at 1 L/min while the water volume is kept constant at 10 L and tilt angle for the PV is maintained at 34°.

Fig. 1



Schematic diagram of PV-TE-MCHP with cooling system.

Table 1

i The presentation of Tables and the formatting of text in the online proof do not match the final output, though the data is the same. To preview the actual presentation, view the Proof.

Dimension of components.

Component	Type	Dimension
PV	Crystalline silicon	675 mm × 85 mm × 2 mm
TEG	Bismuth telluride	40 mm × 40 mm × 4.1 mm
MCHP	Flat plate	750 mm × 60 mm × 3 mm
Water tank	Tower	270 mm × 200 mm × 580 mm
Cooling block	Water	40 mm × 40 mm × 12 mm

3 Experimental details

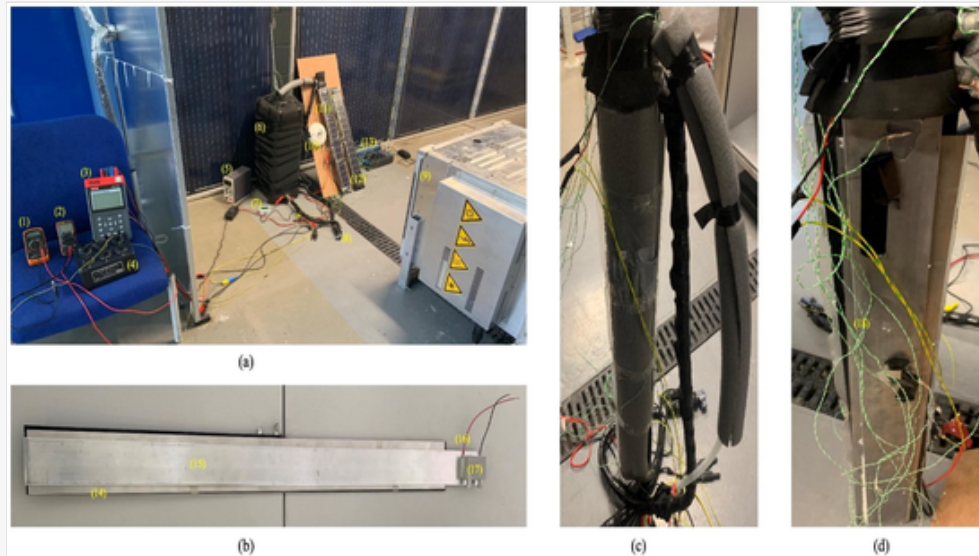
In this section, details amount the experiment are provided and equations to evaluate the performance of the hybrid system are presented.

3.1 Experimental setup

The experimental setup of the PV-TE-MCHP is shown in Fig. 2 and the specification of the components used in the experiment is shown in Table 2. The complete experimental setup can be seen in Fig. 2a which consists of various components such as photovoltaic, thermoelectric generator, flat plate micro-channel heat pipe, solar simulator, pyranometer insulated water tank, direct current (DC) power supply, water pump and water-cooling block. The arrangement of the PV, TEG, MCHP and water-cooling block is shown in Fig. 2b. The pyranometer is used to measure the solar irradiance from the solar simulator while the DC power supply is used to power

the pump. Other measuring instruments include flow meter which measures the flow rate, solar module analyser which is used to measure the electrical performance (open circuit voltage, short circuit current, maximum power, maximum voltage, maximum current and fill factor) of the PV. The electrical performance (voltage and current) of the TEG are measured using a voltmeter and an ammeter. The maximum power output of the thermoelectric generator can be obtained by varying the external load resistance and a resistor box is used for this purpose. The thermoelectric generator used in this study is a commercial TEG (GM250-127-14-16) with 127 pairs of n-type and p-type bismuth telluride thermoelectric legs. A data logger is used to obtain the temperature readings from the K-type thermocouples used which are placed at different locations on the hybrid system. The position of the thermocouples in the experimental setup is shown in [Table 3](#). In this experimental, three thermocouples are used to measure the average temperature of the PV while two thermocouples are used for obtaining the TEG cold side temperature. In addition, one thermocouple is used to obtain the TEG hot side temperature which is the same as the temperature of the MCHP condenser. Furthermore, three thermocouples are used to obtain the average temperature of the water in the tank and an additional thermocouple is used to measure the ambient temperature. The water tank is insulated to present heat loss and two different test cases are considered including PV-TE-MCHP with back surface insulation ([Fig. 2c](#)) and without insulation ([Fig. 2d](#)).

Fig. 2



Experimental test rig showing (a) complete set-up (b) PV-TE-MCHP (c) MCHP with back insulation and (d) MCHP without insulation.

Table 2

i The presentation of Tables and the formatting of text in the online proof do not match the final output, though the data is the same. To preview the actual presentation, view the Proof.

Experimental test rig component specification.

Identifier	Component	Specification	Accuracy	Manufacturer	Quantity
1	Voltmeter	Pocket digital multimeter	±0.5%	Neoteck	1
2	Ammeter	Digital multimeter AN8009	±0.5%	Aneng	1
3	Solar module analyser	ISM 490	±1%	RS Pro	1
4	Resistor box	Variable decade resistor	±1%	Earlywish	1
5	DC power supply	KPS305D	–	Eventek	1
6	Insulated water tank	Tower water tank	–	Tanks direct	1
7	Flow meter	DigiFlow	±5%	Vyair	1
8	Pump	Water pump	–	RS Pro	1
9	Solar simulator	Solar constant MHG 4000/2500	–	Atlas	1
10	Pyranometer	SR20-D2	±1.2%	Hukseflux	1
11	PV-TE-MCHP	–	–	–	1
12	PV only	–	–	–	1
13	Data logger	Memory HiLogger LR8400	–	Hioki	1
14	PV	Unglazed crystalline silicon	–	Guangdong five-star solar energy	1
15	MCHP	Flat plate	–	Guangdong five-star solar energy	1
16	TEG	Peltier module GM250-127-14-16	–	European thermodynamics	1
17	Water cooling block	Aluminium water block	–	Yeeco	1
18	Thermocouple	Type K	±0.5%	RS Pro	16

Table 3

 The presentation of Tables and the formatting of text in the online proof do not match the final output, though the data is the same. To preview the actual presentation, view the Proof.

Position of thermocouples in experimental setup.

Number

Position

PV-TE-MCHP	
1	PV front surface top
2	PV front surface middle
3	PV front surface bottom
4	TEG cold surface right
5	TEG cold surface left
6	TEG hot surface
7	Heat pipe surface middle
8	Water tank bottom
9	Water tank middle
10	Water tank top
11	Cooling block left
12	Cooling block right
13	Ambient temperature
PV only	
14	PV front surface top
15	PV front surface middle
16	PV front surface bottom

3.2 Experimental procedure

An experimental methodology is utilized in this study therefore, the hypothesis that hybrid PV-TE-MCHP can provide enhanced performance compared to conventional PV only is tested experimentally. The experimental setup has been described in the section above while the experimental procedure is described here. This experiment was carried out in a laboratory at the University of Hull, UK in April and the testing were done for several days. The intensity of the solar radiation was varied for different test scenarios and all surfaces except the front surface of the PV were insulated. However, the insulation on the back surface of the MCHP was removed during a test scenario to investigate its effect on the performance of the hybrid system. In addition, a comparison between the performance of the hybrid system and that of the PV only system was made. The electrical performance of the PV was measured every 10 min alongside the voltage and power output of the TEG. Therefore, the solar module analyser and multimeters were used simultaneously to obtain the electrical performance of the PV and TEG at an interval of 10 min. Furthermore, a time interval of 20 s was used to record the temperature readings on the data logger. Depending on the test scenario, the systems were run for several hours to obtain valuable experimental data.

3.3 Evaluation of overall performance

In this section, the equations used to perform the energy and exergy analysis for the PV-TE-MCHP are given.

3.3.1 Energy analysis

The overall power output of the PV-TE-MCHP system is given as,

$$P_{pv-te-mchp} = P_{pv} + P_{te} - P_{pump} \quad (1)$$

where P_{pv} is the power output of the PV, P_{te} is the TE power output and P_{pump} is the power consumed by the pump. Since the flat plate micro-channel heat pipe is a passive device, it does not consume any electricity.

The overall electrical efficiency of the PV-TE-MCHP is given as,

$$\eta_{pv-te-mchp} = \frac{P_{pv} + P_{te} - P_{pump}}{G \times A} \quad (2)$$

where G is the solar radiation and A is the area of the PV cell.

Since the heat removed from the TEG is transported back to the water tank which then increases the temperature of the water, the heating capacity obtained by the water in the tank can be expressed as [42],

$$\dot{Q}_{th} = m_{w_tank} c_w \frac{dT}{dt} \quad (3)$$

where m_{w_tank} is the mass of water tank, c_w is the specific heat capacity of water and \bar{T} is the average temperature of water in the tank.

The thermal efficiency of the system is given as,

$$\eta_{th} = \frac{\int_{t_1}^{t_2} \dot{Q}_{th} dt}{A_c \int_{t_1}^{t_2} G dt} \quad (4)$$

where A_c is the area of the PV collector.

3.3.2 Exergy analysis

The exergy analysis is based on second law of thermodynamics it is used to present the maximum quantity of work that can be produced in a given environment [43]. The exergy efficiency of the PV-TE-MCHP is given as,

$$\eta_{xpvt-te-mchp} = \frac{E_{xpv} + E_{xte} + E_{xw_tank} - P_{pump}}{E_{xin}} \quad (5)$$

where E_{xpv} , E_{xte} are the exergy outputs of PV and TE respectively and E_{xw_tank} is the exergy obtained in the water tank.

$$E_{xpv} = P_{pv} \quad (6)$$

$$E_{xte} = P_{te} \quad (7)$$

Assuming that the temperature value in the water tank is the average of three thermocouple temperature values, E_{xw_tank} can be expressed as [44],

$$E_{xw_tank} = \dot{Q}_{th} \left(1 - \frac{T_a}{T} \right) \quad (8)$$

The exergy from the sun E_{xin} is given as [45],

$$E_{xin} = A_c G \varphi_{srad,max} \quad (9)$$

where $\varphi_{srad,max}$ is the maximum efficiency ratio for determining the exergy of thermal emission at temperature T_{sun} and it is expressed using Petela equation as [46],

$$\varphi_{srad,max} = 1 + \frac{1}{3} \left(\frac{T_a}{T_{sun}} \right)^4 - \frac{4}{3} \frac{T_a}{T_{sun}} \quad (10)$$

where T_a is ambient temperature and T_{sun} is the solar irradiance temperature which is taken as 6000 K [47].

3.4 Error analysis

The experimental error of the corresponding independent variables such as solar radiation, current, voltage and temperature are determined by the accuracy of the measuring instrument used. The relative error (RE) of the dependent variable y is given as [48],

$$RE = \frac{dy}{y} = \frac{\partial f}{\partial x_1} \frac{dx_1}{y} + \frac{\partial f}{\partial x_2} \frac{dx_2}{y} + \dots + \frac{\partial f}{\partial x_n} \frac{dx_n}{y} \quad (11)$$

$$y = f(x_1, x_2, \dots, x_n) \quad (12)$$

where $x_i (i = 1, \dots, n)$ is defined as variable of dependent variable y , and $\frac{\partial f}{\partial x}$ is defined as error transferring coefficient of the variables.

During test period, the experimental relative mean error (RME) is given as,

$$RME = \frac{\sum_1^N |Re|}{N} \quad (13)$$

Using Eqs. (1)–(3), the relative mean error of all the variables are obtained and shown in Table 4. Where T is temperature, G is solar radiation, I is electric current, U is electric voltage, P is power output and η is efficiency.

Table 4

 The presentation of Tables and the formatting of text in the online proof do not match the final output, though the data is the same. To preview the actual presentation, view the Proof.

Experimental relative mean error of variables.

Variable	T	G	I	U	P	η
RME	0.33%	2%	±1%	±1%	±2%	±4%

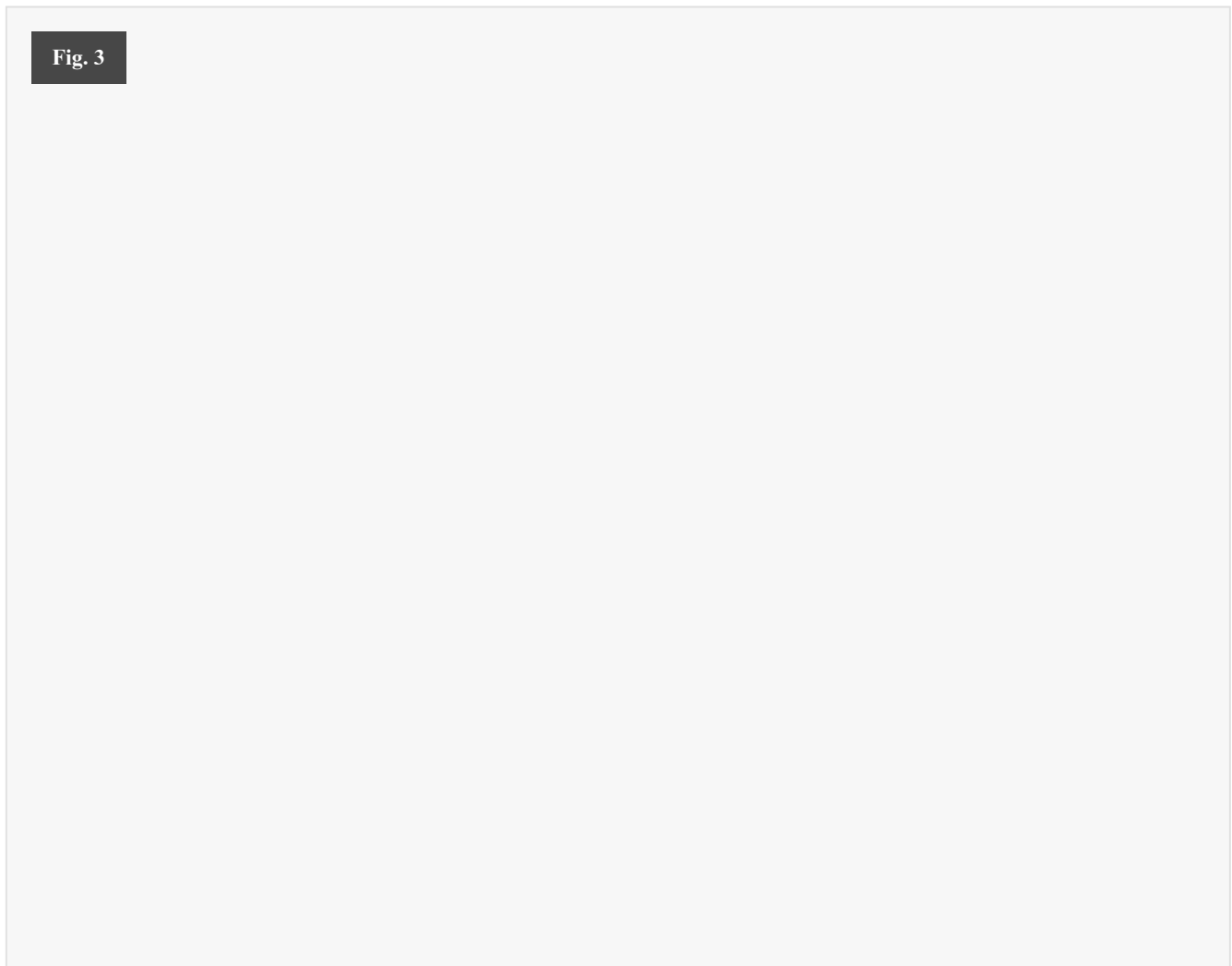
4 Results and discussion

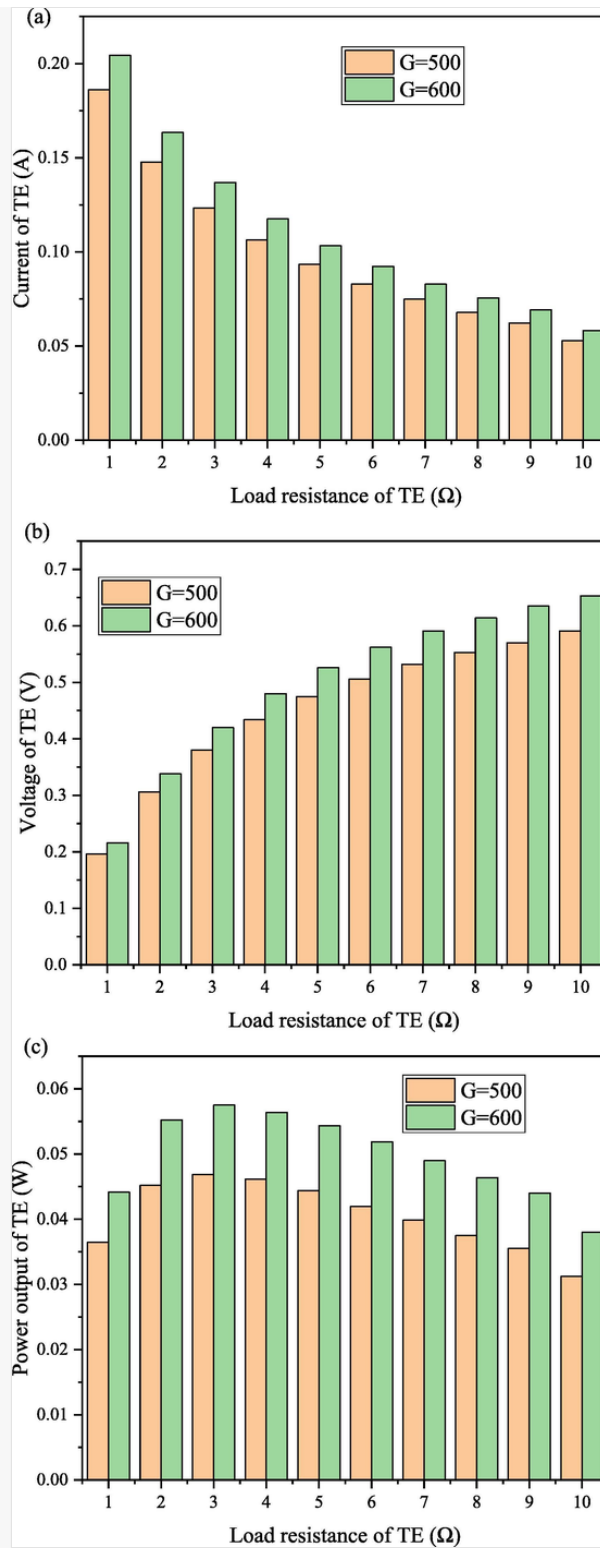
The results from this study are presented in this section and analysed in detail. The experiment was carried out under laboratory conditions and the solar radiation is varied using a solar simulator.

4.1 Effect of thermoelectric load resistance

The maximum power output of the thermoelectric generator can be obtained by impedance matching. Therefore, the external load resistance can be varied to obtain the maximum power output. Fig. 3 shows the variation of load resistance with the current, voltage and power output of the TE in the hybrid system. The experiment was conducted using two different solar radiation values and the results obtained are shown in Fig. 3. It can be seen from Fig. 3a that the current of the thermoelectric decreases rapidly as the load resistance increases however, the voltage of the thermoelectric shows an opposing trend. A better understanding of the effect of external load resistance on thermoelectric power output is shown in Fig. 3c. It can be seen that the power output firstly increases before decreasing as the load resistance is varied from 1 Ω to 10 Ω . In fact, the maximum power output of the thermoelectric is obtained at a load resistance value of 3 Ω . Therefore, it is important to investigate the optimum load resistance at which maximum power output can be obtained. In addition, it can be seen from Fig. 3c that the power output increases as the solar radiation increases because of the increase in absorbed energy by the thermoelectric and the greater temperature difference. The results Furthermore, the result in Fig. 3b shows the rising tendency of the thermoelectric voltage as the load resistance is increased.

Fig. 3





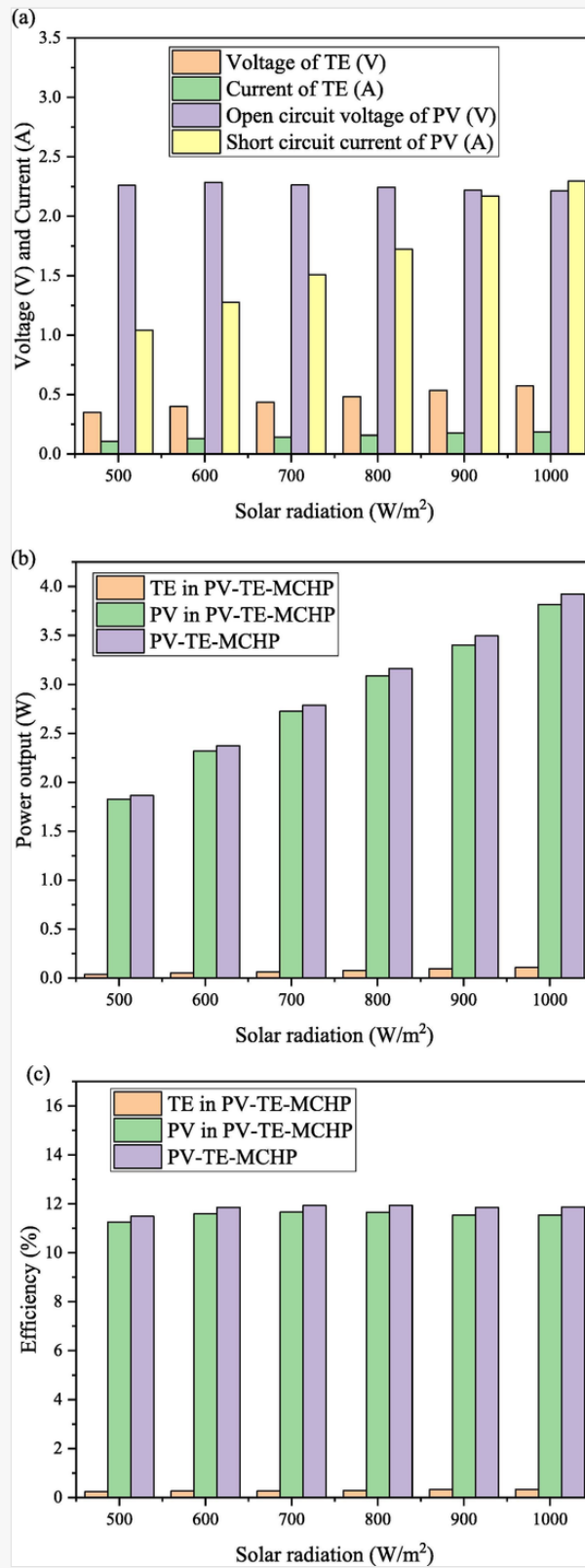
Variation of load resistance with (a) current (b) voltage and (c) power output of TE.

4.2 Effect of solar radiation

The solar radiation is one of the most important parameters that significantly affects the performance of the hybrid system. Therefore, the effect of solar radiation variation on PV-TE-MCHP electrical performance is shown in Fig. 4. It can be seen from Fig. 4a that the open circuit voltage and short circuit current of the PV in

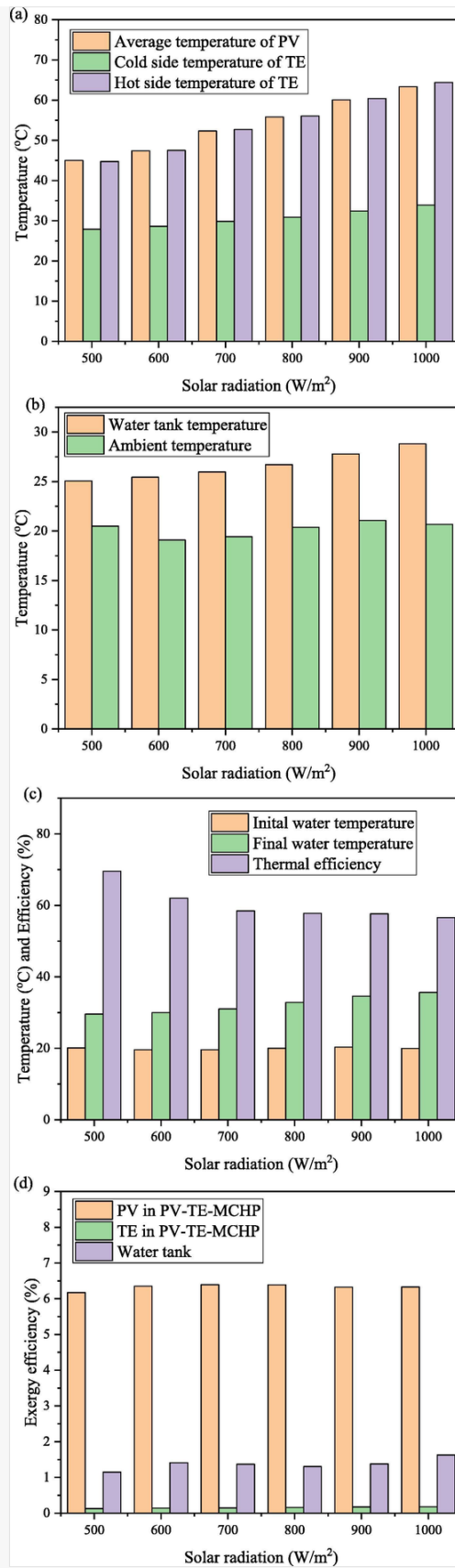
the hybrid system show an opposing trend as the solar radiation is varied from 500 W/m^2 to 1000 W/m^2 . While the short circuit current increases rapidly, the open circuit voltage decreases slowly as the radiation increases. In addition, it can be seen from Fig. 4a that the voltage and current of the thermoelectric increases as the solar radiation increases. This shows that the PV and TE have a complex relationship as the photovoltaic performance (efficiency) decreases under high radiation values while that of the TE increases under high radiation values. Furthermore, the average power output of the hybrid system is shown in Fig. 4b. As expected, the power output of the hybrid system increases as the solar radiation increases. It is also important to note that the PV provides the greater percentage of the overall power output of the hybrid system. The power output of the PV-TE-MCHP increases from 1.86 W to 3.92 W as the solar radiation increases from 500 W/m^2 to 1000 W/m^2 . Therefore, increased power output can be obtained from the hybrid system at high radiation values. However, the efficiency of the hybrid system decreases as the solar radiation increases as shown in Fig. 4c. This can be explained by the increase in average PV temperature as the solar radiation increases as shown in Fig. 5a. An increase in temperature of PV generally leads to a decrease in efficiency. In addition, Fig. 5a shows the temperature of the TE hot side increases rapidly with solar radiation increase and the cold side temperature also increases. The reason for the increase in cold side temperature is that the heat removed from the TE cold side is transported to the water tank, which is also recirculated back to the TE. As shown in Fig. 5b, the temperature of water in the tank also increases as the solar radiation increases. Furthermore, the ambient temperature values recorded for the different test days the solar radiation was varied is shown in Fig. 5b. The initial and final temperature of the water in the tank after a 5 h period is shown in Fig. 5c. The hybrid system was run under a constant radiation value for 5 h to investigate the capacity of the system to increase the water temperature in the tank. In addition, the thermal efficiency of the system is calculated and shown in Fig. 5c. It can be seen that the thermal efficiency gradually decrease as the solar radiation increase. This is because, although the difference between the initial and final water temperature increase with solar radiation increase, this difference is not significant enough to compensate for the increased solar energy absorbed therefore, the thermal efficiency which is a ratio between the useful thermal energy output and the input energy decreased as the solar radiation increased. Nevertheless, it can be seen from Fig. 5c that the highest thermal efficiency of 69.53% is obtained for the day the system was run under a solar radiation value of 500 W/m^2 . The lowest thermal efficiency value obtained is 56.57%, which is still very high thereby demonstrating the feasibility of the hybrid system for water heating and electricity production. Furthermore, the exergy of the PV, TE and water tank in the hybrid system is calculated and shown in Fig. 5d. It can be seen that the exergy of the TE in PV-TE-MCHP is very low although it increases from 0.13% to 0.18% as the solar radiation increases from 500 W/m^2 to 1000 W/m^2 . In addition, the highest exergy efficiency of the PV in PV-TE-MCHP was 6.39% under a solar radiation of 700 W/m^2 . The exergy efficiency of the PV and TE in the hybrid system are lower than their corresponding electrical efficiency because for the exergy efficiency calculation, the collector area is used while the PV cell area is used for the electrical efficiency calculation because the PV cells do not completely cover the surface. Furthermore, it can be seen from Fig. 5d that the highest exergy efficiency obtained from the water tank is 1.63% at a solar radiation of 1000 W/m^2 . The water tank exergy efficiency is highly dependent on the thermal efficiency and the environmental conditions especially the ambient temperature.

Fig. 4



Solar radiation variation with (a) voltage, current (b) power output and (c) efficiency.

Fig. 5



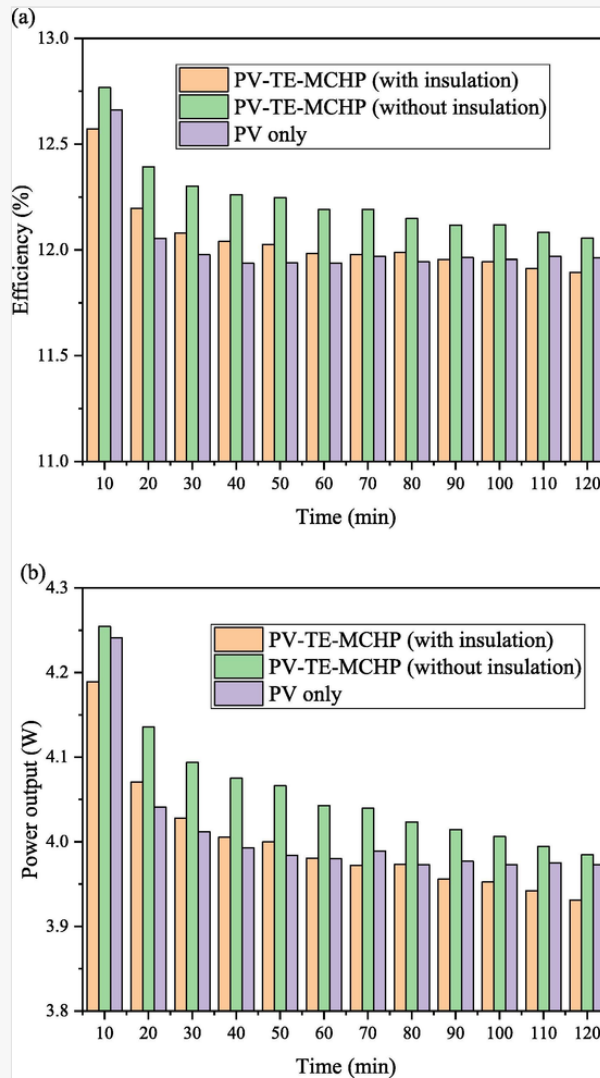
Variation of solar radiation with (a) PV, TE temperature (b) water tank, ambient temperature, (c) thermal efficiency and (d) exergy efficiency.

4.3 Effect of insulation and comparison with photovoltaic only

To study the effect of insulation at the back surface of the MCHP on the performance of the hybrid system, two different cases were compared as shown in Fig. 2c and Fig. 2d respectively and the results obtained were compared to those of a PV only system. It can be seen from Fig. 6a that the presence of insulation at the back of the MCHP significantly lowers the efficiency of the hybrid system. The reason for this is that the presence of insulation at the rear of the micro-channel heat pipe contributes to the additional increase of the photovoltaic temperature. In fact, after running the system for 1 h, the efficiency of the hybrid system with and without insulation is 11.98% and 12.19% respectively. In comparison, the efficiency of the PV only at that time is 11.94% thereby showing the advantage of the hybrid system over PV only system. In addition, as expected the efficiency of the hybrid system with and without insulation and that of the PV all decrease as the running time increases as shown in Fig. 6a due to the increase in operating temperature. Consequently, effective thermal management of photovoltaic is essential for maintaining high conversion efficiency during long operational period. Furthermore, Fig. 6a shows that the advantage of the hybrid system with insulation over PV only system is lost after running the system for long period because of the ineffectiveness of the cooling system due to the increase in the water temperature in the tank. Therefore, the temperature of the cooling water in the tank must be maintained at a low value by introducing fresh cold water if only high electrical conversion efficiency is desired. Fig. 6b shows that the PV-TE-MCHP without insulation provides the highest power output compared to the other systems. It can also be seen that the power output of the PV only stabilises after some time while those of the PV-TE-MCHP with and without insulation continues to decrease due to the ineffectiveness of the cooling system after a long period of time. Consequently, there has to be a trade-off between obtaining increased power output or efficiency from the hybrid system and obtaining additional hot water as a by-product. The average temperature of the PV in the PV-TE-MCHP with and without insulation and the PV only is shown in Fig. 7a. It can be seen clearly that the temperature of the PV in the PV only system is the highest therefore; the effectiveness of the hybrid system in providing reduced PV temperature is demonstrated. In fact, after running the system for 1 h, the PV temperature in the hybrid system with and without insulation is 62.2 °C and 61.9 °C respectively. In comparison, the temperature of the PV in PV only at that time is 67.9 °C. Therefore, it can be concluded that the PV-TE-MCHP without insulation provides the lowest PV temperature. This is significant because there is an inverse relationship between the temperature and photovoltaic efficiency. Furthermore, the temperature difference across the hot and cold sides of the thermoelectric in the PV-TE-MCHP with and without insulation is shown in Fig. 7b. As expected, the temperature difference of the TE in PV-TE-MCHP with insulation is higher than that without insulation due to the heat loss from absence of insulation. However, the contribution of the TE to the overall power output and efficiency of the hybrid system is not that significant to warrant the use of insulation. In addition, it can be seen that the thermoelectric temperature difference gradually decrease as the time increase due to the reduction in the cooling effectiveness of the water tank with time. Similarly, as shown in Fig. 7c, the temperature of the water in the tank when an insulation is used in the PV-TE-MCHP is higher than that without insulation because of better prevention of heat loss. Consequently, if water heating is the main requirement of the hybrid system, an insulation should be used, however, if enhanced electricity generation is desired, insulation should not be used on the back surface of the micro-channel heat pipe. There is a direct relationship between the thermoelectric temperature difference and the water tank temperature because the water tank provides the

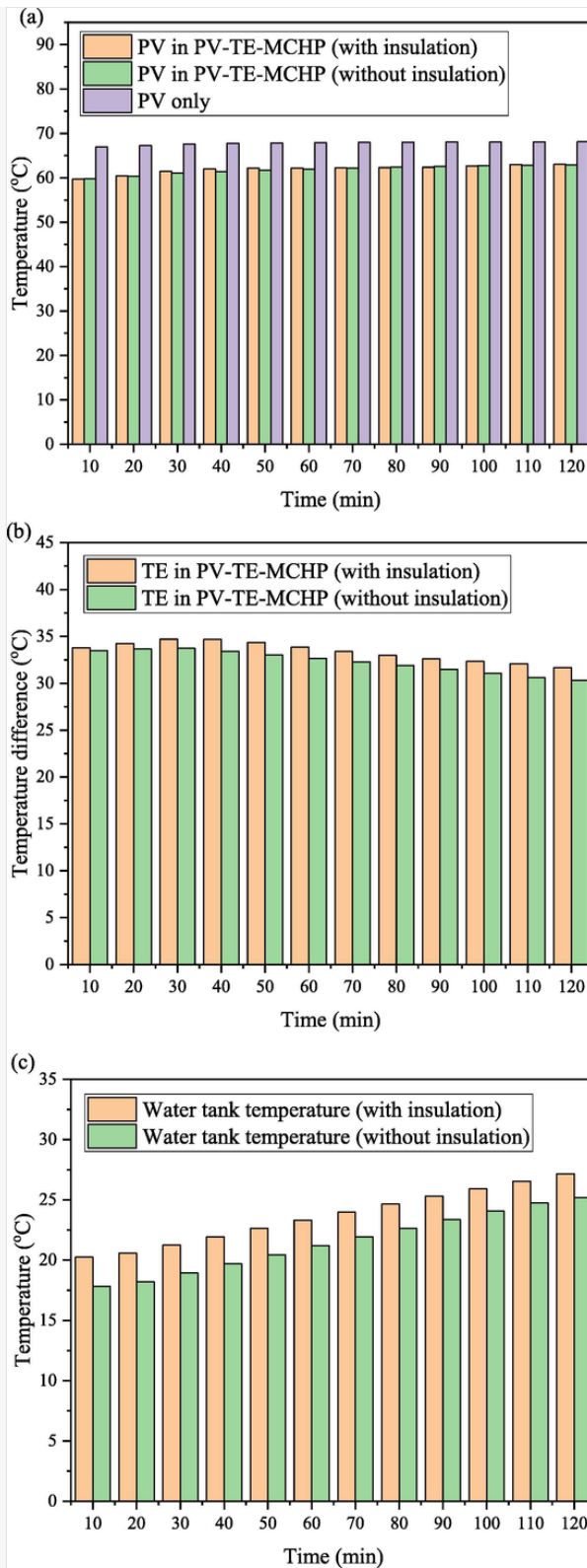
cooling water for the thermoelectric cold side. Therefore, as the thermoelectric temperature difference in the hybrid systems decrease with increase in time (Fig. 7b), the water tank temperature increase (Fig. 7c). This means that the water tank is no longer effectively removing the waste heat from the thermoelectric cold side thus, the TE temperature difference decreases.

Fig. 6



Time variation with (a) efficiency and (b) power output.

Fig. 7



Time variation with (a) PV temperature (b) TE temperature difference and (c) water tank temperature.

5 Conclusion

A detailed experimental investigation of a photovoltaic-thermoelectric with flat plate micro-channel heat pipe and water-cooling was presented in this study for the first time. This study filled the gap identified in the

detailed literature review conducted. Furthermore, the feasibility of hybrid PV-TE with heat pipe for power generation and hot water production was demonstrated in this study for the first time. Using a solar simulator, solar radiation was varied for different test scenarios and exergy analysis was performed. The effect of thermoelectric load resistance, insulation layer on the backside of the flat plate-micro-channel heat pipe and solar radiation on the performance of the hybrid system was presented and a comparison with a photovoltaic only system was made. A detailed explanation of the experimental procedure and components was provided, and the experiment was carried out in a laboratory at the University of Hull, United Kingdom in April. The advantage of the experimental study is that all the results provided can be used for real applications. The experimental study was conducted under similar conditions as would be found in real application of the hybrid system. The main conclusions from this study are:

- 1) The efficiencies of the photovoltaic-thermoelectric-microchannel heat pipe with and without insulation and that of the photovoltaic only after 1 h were 11.98%, 12.19% and 11.94% respectively. Therefore, the hybrid system provided an enhanced performance.
- 2) There has to be a trade-off between obtaining increased power output or efficiency from the hybrid system and obtaining additional hot water as a by-product.
- 3) The photovoltaic temperature in the hybrid system with and without insulation (62.2 °C and 61.9 °C respectively) was lower than that in the photovoltaic only system (67.9 °C) after 1 h.
- 4) There is an optimum load resistance for obtaining maximum power output from the thermoelectric generator.
- 5) The average power output of the hybrid system increased from 1.86 W to 3.92 W when the solar radiation increased from 500 W/m² to 1000 W/m².
- 6) The highest and lowest thermal efficiencies obtained were 69.53% and 56.57% respectively under certain conditions.

CRedit authorship contribution statement

Samson Shittu: Conceptualization, Investigation, Writing - original draft, Writing - review & editing. **Guiqiang Li:** Investigation, Writing - review & editing, Project administration. **Xudong Zhao:** Funding acquisition. **Jinzi Zhou:** Investigation. **Xiaoli Ma:** Supervision. **Yousef Golizadeh Akhlaghi:** Investigation.

Declaration of Competing Interest

The authors declare that they have no known competing financial interests or personal relationships that could have appeared to influence the work reported in this paper.

Acknowledgement

This study was sponsored by the Project of EU Marie Curie International incoming Fellowships Program (745614). The authors would also like to express our appreciation for the financial supports from EPSRC (EP/R004684/1) and Innovate UK (TSB 70507-481546) for the Newton Fund - China-UK Research and Innovation Bridges Competition 2015 Project 'A High Efficiency, Low Cost and Building Integrate-able Solar

References

 The corrections made in this section will be reviewed and approved by journal production editor.

- [1] Shittu S., Li G., Zhao X., Ma X., Akhlaghi Y.G., Fan Y. Comprehensive study and optimization of concentrated photovoltaic-thermoelectric considering all contact resistances. *Energy Convers Manag* 2020;205:112422. doi:10.1016/j.enconman.2019.112422.
- [2] Li G, Ma X, Shittu S, Zhao X. Solar thermoelectric technologies for power generation. In: Zhao X, Ma X, editors. *Adv. Energy Effic. Technol. Sol. Heating, Cool. Power Gener.*, Cham: Springer International Publishing; 2019, p. 341–71. doi:10.1007/978-3-030-17283-1_10.
- [3] Parida B., Iniyani S., Goic R. A review of solar photovoltaic technologies. *Renew Sustain Energy Rev* 2011;15:1625–1636. doi:10.1016/j.rser.2010.11.032.
- [4] Zhang X., Zhao X., Smith S., Xu J., Yu X. Review of R&D progress and practical application of the solar photovoltaic/thermal (PV/T) technologies. *Renew Sustain Energy Rev* 2012;16:599–617.
- [5] Skoplaki E., Palyvos J.A. On the temperature dependence of photovoltaic module electrical performance: a review of efficiency/power correlations. *Sol Energy* 2009;83:614–624. doi:10.1016/j.solener.2008.10.008.
- [6] Shittu S., Li G., Zhao X., Ma X. Series of detail comparison and optimization of thermoelectric element geometry considering the PV effect. *Renew Energy* 2019;130:930–942. doi:10.1016/j.renene.2018.07.002.
- [7] Li G., Shittu S., Zhao X., Ma X. Preliminary experiment on a novel photovoltaic-thermoelectric system in summer. *Energy* 2019;188:116041. doi:10.1016/j.energy.2019.116041.
- [8] Shittu S., Li G., Zhao X., Ma X., Akhlaghi Y.G., Ayodele E. Optimized high performance thermoelectric generator with combined segmented and asymmetrical legs under pulsed heat input power. *J Power Sources* 2019;428:53–66. doi:10.1016/j.jpowsour.2019.04.099.
- [9] Rowe D.M. Thermoelectrics, an environmentally-friendly source of electrical power. *Renew Energy* 1999;16:1251–1256. doi:10.1016/S0960-1481(98)00512-6.
- [10] Shittu S., Li G., Zhao X., Ma X., Akhlaghi Y.G., Ayodele E. High performance and thermal stress analysis of a segmented annular thermoelectric generator. *Energy Convers Manag* 2019;184:180–193. doi:10.1016/j.enconman.2019.01.064.

- [11] Li G., Shittu S., Ma X., Zhao X. Comparative analysis of thermoelectric elements optimum geometry between Photovoltaic-thermoelectric and solar thermoelectric. *Energy* 2019;171:599–610. doi:10.1016/j.energy.2019.01.057.
- [12] Li G., Zhao X., Jin Y., Chen X., Ji J., Shittu S. Performance analysis and discussion on the thermoelectric element footprint for PV–TE maximum power generation. *J Electron Mater* 2018;47:5344–5351.
- [13] Li G., Chen X., Jin Y. Analysis of the primary constraint conditions of an efficient photovoltaic-thermoelectric hybrid system. *Energies* 2017;10.. doi:10.3390/en10010020.
- [14] Shittu S., Li G., Akhlaghi Y.G., Ma X., Zhao X., Ayodele E. Advancements in thermoelectric generators for enhanced hybrid photovoltaic system performance. *Renew Sustain Energy Rev* 2019;109:24–54. doi:10.1016/j.rser.2019.04.023.
- [15] Li G., Shittu S., Diallo T.M.O., Yu M., Zhao X., Ji J. A review of solar photovoltaic-thermoelectric hybrid system for electricity generation. *Energy* 2018;158:41–58. doi:10.1016/j.energy.2018.06.021.
- [16] Narducci D, Bermel P, Lorenzi B, Wang N. Hybrid and fully thermoelectric solar harvesting. 1st ed. Switzerland: Springer International Publishing; 2018. doi:10.1109/IPDPS.2006.1639640.
- [17] Huen P., Daoud W.A. Advances in hybrid solar photovoltaic and thermoelectric generators. *Renew Sustain Energy Rev* 2017;72:1295–1302. doi:10.1016/j.rser.2016.10.042.
- [18] Yin E., Li Q., Xuan Y. A novel optimal design method for concentration spectrum splitting photovoltaic-thermoelectric hybrid system. *Energy* 2018;163:519–532. doi:10.1016/j.apenergy.2018.05.127.
- [19] Li G., Zhou K., Song Z., Zhao X., Ji J. Inconsistent phenomenon of thermoelectric load resistance for photovoltaic–thermoelectric module. *Energy Convers Manag* 2018;161:155–161. doi:10.1016/j.enconman.2018.01.079.
- [20] Babu C., Ponnambalam P. The theoretical performance evaluation of hybrid PV-TEG system. *Energy Convers Manag* 2018;173:450–460. doi:10.1016/j.enconman.2018.07.104.
- [21] Mahmoudinezhad S., Rezaia A., Rosendahl L.A. Behavior of hybrid concentrated photovoltaic-thermoelectric generator under variable solar radiation. *Energy Convers Manag* 2018;164:443–452. doi:10.1016/j.enconman.2018.03.025.
- [22] Zhang J., Xuan Y., Yang L. Performance estimation of photovoltaic-thermoelectric hybrid systems. *Energy* 2014;78:895–903. doi:10.1016/j.energy.2014.10.087.
- [23] Singh S., Ibeagwu O.I., Lamba R. Thermodynamic evaluation of irreversibility and optimum performance of a concentrated PV-TEG cogenerated hybrid system. *Sol Energy* 2018;170:896–905. doi:10.1016/j.solener.2018.06.034.

- [24] Rezanian A., Rosendahl L.A. Feasibility and parametric evaluation of hybrid concentrated photovoltaic-thermoelectric system. *Appl Energy* 2017;187:380–389. doi:10.1016/j.apenergy.2016.11.064.
- [25] Fallah Kohan H.R., Lotfipour F., Eslami M. Numerical simulation of a photovoltaic thermoelectric hybrid power generation system. *Sol Energy* 2018;174:537–548. doi:10.1016/j.solener.2018.09.046.
- [26] Motiei P., Yaghoubi M., GoshtashbiRad E., Vadiee A. Two-dimensional unsteady state performance analysis of a hybrid photovoltaic-thermoelectric generator. *Renew Energy* 2018;119:551–565. doi:10.1016/j.renene.2017.11.092.
- [27] Li D., Xuan Y., Li Q., Hong H. Exergy and energy analysis of photovoltaic-thermoelectric hybrid systems. *Energy* 2017;126:343–351. doi:10.1016/j.energy.2017.03.042.
- [28] Yang Z., Li W., Chen X., Su S., Lin G., Chen J. Maximum efficiency and parametric optimum selection of a concentrated solar spectrum splitting photovoltaic cell-thermoelectric generator system. *Energy Convers Manag* 2018;174:65–71. doi:10.1016/j.enconman.2018.08.038.
- [29] Kossyvakis D.N., Voutsinas G.D., Hristoforou E.V. Experimental analysis and performance evaluation of a tandem photovoltaic-thermoelectric hybrid system. *Energy Convers Manag* 2016;117:490–500. doi:10.1016/j.enconman.2016.03.023.
- [30] Zhang J., Xuan Y. An integrated design of the photovoltaic-thermoelectric hybrid system. *Sol Energy* 2019;177:293–298. doi:10.1016/j.solener.2018.11.012.
- [31] Cui T., Xuan Y., Yin E., Li Q., Li D. Experimental investigation on potential of a concentrated photovoltaic-thermoelectric system with phase change materials. *Energy* 2017;122:94–102. doi:10.1016/j.energy.2017.01.087.
- [32] Darkwa J., Calautit J., Du D., Kokogianakis G. A numerical and experimental analysis of an integrated TEG-PCM power enhancement system for photovoltaic cells. *Appl Energy* 2019;248:688–701. doi:10.1016/j.apenergy.2019.04.147.
- [33] Mahmoudinezhad S., Atouei S.A., Cotfas P.A., Cotfas D.T., Rosendahl L.A., Rezanian A. Experimental and numerical study on the transient behavior of multi-junction solar cell-thermoelectric generator hybrid system. *Energy Convers Manag* 2019;184:448–455. doi:10.1016/j.enconman.2019.01.081.
- [34] Yin E., Li Q., Xuan Y. Experimental optimization of operating conditions for concentrating photovoltaic-thermoelectric hybrid system. *J Power Sources* 2019;422:25–32. doi:10.1016/j.jpowsour.2019.03.034.
- [35] Li G., Diallo T.M.O., Akhlaghi Y.G., Shittu S., Zhao X., Ma X., et al Simulation and experiment on thermal performance of a micro-channel heat pipe under different evaporator temperatures

and tilt angles. *Energy* 2019;179:549–557. doi:10.1016/j.energy.2019.05.040.

- [36] Li G., Zhang G., He W., Ji J., Lv S., Chen X., et al Performance analysis on a solar concentrating thermoelectric generator using the micro-channel heat pipe array. *Energy Convers Manag* 2016;112:191–198. doi:10.1016/j.enconman.2016.01.025.
- [37] Lv S., He W., Hu D., Zhu J., Li G., Chen H., et al Study on a high-performance solar thermoelectric system for combined heat and power. *Energy Convers Manag* 2017;143:459–469. doi:10.1016/j.enconman.2017.04.027.
- [38] Li G., Feng W., Jin Y., Chen X., Ji J. Discussion on the solar concentrating thermoelectric generation using micro-channel heat pipe array. *Heat Mass Transf* 2017;53:3249–3256. doi:10.1007/s00231-017-2026-3.
- [39] Makki A., Omer S., Su Y., Sabir H. Numerical investigation of heat pipe-based photovoltaic-thermoelectric generator (HP-PV/TEG) hybrid system. *Energy Convers Manag* 2016;112:274–287. doi:10.1016/j.enconman.2015.12.069.
- [40] Li G., Zhao X., Ji J. Conceptual development of a novel photovoltaic-thermoelectric system and preliminary economic analysis. *Energy Convers Manag* 2016;126:935–943. doi:10.1016/j.enconman.2016.08.074.
- [41] Shittu S., Li G., Zhao X., Akhlaghi Y.G., Ma X., Yu M. Comparative study of a concentrated photovoltaic-thermoelectric system with and without flat plate heat pipe. *Energy Convers Manag* 2019;193:1–14. doi:10.1016/j.enconman.2019.04.055.
- [42] Li G., Pei G., Ji J., Yang M., Su Y., Xu N. Numerical and experimental study on a PV/T system with static miniature solar concentrator. *Sol Energy* 2015;120:565–574. doi:10.1016/j.solener.2015.07.046.
- [43] Chow T.T., Pei G., Fong K.F., Lin Z., Chan A.L.S., Ji J. Energy and exergy analysis of photovoltaic-thermal collector with and without glass cover. *Appl Energy* 2009;86:310–316. doi:10.1016/j.apenergy.2008.04.016.
- [44] Gang P., Guiqiang L., Xi Z., Jie J., Yuehong S. Experimental study and exergetic analysis of a CPC-type solar water heater system using higher-temperature circulation in winter. *Sol Energy* 2012;86:1280–1286. doi:10.1016/j.solener.2012.01.019.
- [45] Gang P., Huide F., Tao Z., Jie J. A numerical and experimental study on a heat pipe PV/T system. *Sol Energy* 2011;85:911–921. doi:10.1016/j.solener.2011.02.006.
- [46] Petela R. Exergy of undiluted thermal radiation. *Sol Energy* 2003;74:469–488. doi:10.1016/S0038-092X(03)00226-3.
- [47] Li G., Ji J., Zhang G., He W., Chen X., Chen H. Performance analysis on a novel micro-channel heat pipe evacuated tube solar collector-incorporated thermoelectric generation. *Int J Energy Res*

2016;40:2117–2127. doi:10.1002/er.3589.

[48] Ji J., He H., Chow T., Pei G., He W., Liu K. Distributed dynamic modeling and experimental study of PV evaporator in a PV/T solar-assisted heat pump. *Int J Heat Mass Transf* 2009;52:1365–1373. doi:10.1016/j.ijheatmasstransfer.2008.08.017.

Highlights

- Photovoltaic-thermoelectric with flat plate micro-channel heat pipe is presented.
 - Energy and exergy analysis of the hybrid system is performed.
 - Comparison is made between the hybrid system and photovoltaic only system.
 - Feasibility of the hybrid system is demonstrated experimentally.
-

Queries and Answers

Query: Your article is registered as a regular item and is being processed for inclusion in a regular issue of the journal.

If this is NOT correct and your article belongs to a Special Issue/Collection please contact

J.Shanmugam@elsevier.com immediately prior to returning your corrections.

Answer: Yes

Query: The author names have been tagged as given names and surnames (surnames are highlighted in teal color).

Please confirm if they have been identified correctly.

Answer: Yes

Query: Please check the sentence “The results”, it seems to be incomplete, and correct if necessary.

Answer: Thank you. Kindly see the completed sentence already edited in the manuscript:

Furthermore, the result in Fig. 3b shows the rising tendency of the thermoelectric voltage as the load resistance is increased.

Query: Have we correctly interpreted the following funding source(s) and country names you cited in your article: UK Research and Innovation, United Kingdom; Marie Curie, United Kingdom; Newton Fund, United Kingdom; Innovate

UK, United Kingdom; EPSRC, United Kingdom; TSB, United Kingdom? /

Answer: Yes